ARTICLE NO. 79-4099

Triple-Point Pressure Evaporation of Impacted Droplets

James J. Rizza*
California State University, Fullerton, Calif.

The spray evaporator is a heat rejection device used for thermal control of spacecraft. An expendable evaporant is used to cool a transport fluid by means of evaporative cooling. The evaporant is sprayed at vacuum conditions onto a warm, highly conductive surface and is evaporated. The vapor is then vented to space. An important aspect of the evaporator is the way in which the droplets impact and evaporate on the warm evaporator surface in a near-vacuum environment. A high-speed photographic study was made to observe the impact and evaporation of water droplets at pressures below the triple-point pressure of water. The droplets ranged in size from 50μ to 600μ in diameter. Surface temperatures ranged from 140°F to 35°F. It was determined from observations of the high-speed films that the degree of solidification before impact determines the impact mechanism to a large degree, and that the surface temperature determines the evaporation and wetting mechanism, while the other prameters have only a secondary effect on the system.

Introduction

THE evaporation of impacted droplets has received considerable attention in the literature for evaporation pressure ranges above the triple-point. How liquid droplets impact and evaporate on warm surfaces is of interest in a number of areas of engineering, e.g., spray evaporators, cooling of turbine blades, and the cooling of hot metal ingots, to name a few. The Leidenfrost phenomenon has been studied for a number of years.[1] The prediction of the transition Leidenfrost temperature is of current importance in fast breeder liquid-metal cooled reactors and in cryogenic systems.[2] Evaporation of impacted droplets below the Leidenfrost transition temperature has also been studied for a number of years, although not to the same degree as the Leidenfrost phenomenon.[3,4]

The present investigation is a study of the evaporation of impacted water droplets at pressures near or below the triple-point pressure and at temperatures below the Leidenfrost transition temperature. Table 1 lists the important parameters for the study. The high-speed camera and lighting were external to the environmental chamber. The camera was positioned 17 in. from the evaporating surface. The view angle was 5 deg above the evaporating surface for the impact mechanism studies and 45 deg above the surface for the evaporation mechanism studies. The impact mechanism was studied at a film speed of 6000 frames/s and the evaporation mechanism was studied at a film speed of 600 frames/s.

Impact Mechanism

The photograph studies reveal that the degree of droplet solidification before impact determines to a large degree the type of impact mechanism that occurs. It can be demonstrated that the degree of solidification is dependent on droplet size, exposure time, and chamber pressure. When a liquid droplet is suddenly exposed to an ambient pressure below its triple-point pressure, evaporative cooling and then freezing of the droplet occurs. By performing an energy and mass balance on the evaporating droplet, a relationship for the droplet freezing times as a function of droplet size and chamber pressure can be found.[5]

The exact solution of a freezing droplet is a multidimensional problem. The temperature field within the droplet varies spatially and with time. If the internal thermal resistance of the droplet can be neglected, the problem reduces to a one-dimensional problem. Although the conductivity of water is poor, the sublimation rates are low and the droplet diameters are typically small. Therefore, it can be shown that the ratio of external thermal resistance to internal thermal resistance is low, and the spatial variation of temperature can be neglected within the droplet.

The rate of evaporation from the surface is a function of the vapor pressure and temperature of the liquid and is given by the following relation:

$$\mathrm{d}m/\mathrm{d}t=\sigma A P_v (M/2\pi RT)^{1/2} \tag{1}$$

where σ is the evaporation coefficient and m, t, A, P_v, M, R, and T are the mass, time, surface area, vapor pressure, molecular weight, gas constant, and temperature, respectively.[5] A similar expression can be written for the condensation rate. The net loss of mass for the droplet during the liquid state is

$$\mathrm{d}m/\mathrm{d}t=\sigma A (P_v-P_0)(M/2\pi RT)^{1/2} \tag{2}$$

where P_0 is the ambient pressure.

During evaporative cooling, the energy required to evaporate the liquid at the surface of the droplet comes from the internal energy of the droplet, i.e.

$$Q=(m_0-\tfrac{1}{2}m_{gl})C_p\Delta T \tag{3}$$

where Q is the heat transferred, m_{gl} is the mass which is evaporated, m_0 is the initial mass, and ΔT is the temperature difference between the initial and triple-point temperatures. The term $(m_0-\tfrac{1}{2}m_{gl})$ is the average droplet mass during this vaporization stage. The heat transferred is also equal to the evaporation energy,

$$Q=m_{gl}h_{fg} \tag{4}$$

where h_{fg} is the heat of vaporization. Combining Eqs. (3) and (4) gives the following equation:

$$m_{gl}=\frac{m_0}{\tfrac{1}{2}+h_{fg}/C_p\Delta T} \tag{5}$$

Received June 6, 1978; revision received Jan. 9, 1979.

Index categories: Spacecraft Temperature Control; Thermal Control; Thermophysical Properties of Matter.

*Professor and Chair of Mechanical Engineering. Member AIAA.

During the freezing process, the energy required for vaporization comes from the heat of fusion denoted by h_{ig} and therefore

$$m_{g2}h_{fg} = (m_I - m_{g2})h_{ig} \tag{6}$$

where m_I is the mass of the droplet after cooling to the triple-point temperature and m_{g2} is the mass which is vaporized during the freezing process. Also, note that

$$m_I = m_0 - m_{gI} \tag{7}$$

and

$$m_g = m_{gI} + m_{g2} \tag{8}$$

where m_g is the total mass evaporated during cooling and freezing states. Combining Eqs. (5-8) gives the ratio between total mass evaporated and the initial mass

$$\frac{m_g}{m_0} = \left(\frac{h_{fg}}{h_{ig}} + I\right)^{-I} + \frac{I - (h_{fg}/h_{ig} + I)^{-I}}{½ + h_{fg}/C_p\Delta T} \tag{9}$$

Thus, the percentage of mass evaporated is a function of the initial temperature only. If the initial temperature of a water droplet is 100°F, then 17% of the droplet vaporizes during the cooling to the triple-point temperature and the freezing of the droplet. If the initial temperature is 40°F, then 12% of the droplet vaporizes. Therefore, the freezing times are relatively insensitive to the initial evaporant temperature. In Ref. 5, Eqs. (2) and (9) are solved to obtain the freezing times. The freezing times, θ, are proportional to the following parameters:

$$\theta \sim (m_g/m_0)(d/\sigma)(P_{0t} - P_0)^{-I} \tag{10}$$

where P_{0t} denotes the triple-point pressure and d is the droplet diameter. Figure 1 gives the freezing times in seconds for a 100μ, 200μ, and 400μ water droplet for the ratio of ambient to triple-point pressure based on the solution to Eqs. (2) and (9).

Typical exposure time for small droplets during the test was .05 s and typical chamber pressure was 3.6 mm Hg. Thus, from Fig. 1, droplets smaller than 40μ in diameter would be totally frozen, while droplets smaller than 75μ would be at least 50% frozen on a mass basis, or 20% of the outer diameter of the droplet would be frozen. At the lowest chamber pressure of the test, (i.e., 1.4 mm Hg) from Fig. 1, liquid droplets smaller than 95μ in diameter would be totally frozen and droplets smaller than 200μ would have at least 20% of their outer diameter frozen. The information given in Fig. 1 tends to predict shorter freezing times than those observed in the photographic study. This is due in part to neglecting the internal thermal resistance of the droplets in the above development. However, the freezing rates presented in Fig. 1 are representative of the rate observed in the photographic study for the range of chamber pressures considered during the testing.

Table 1 Test parameters

Parameter	Range	Usual value
Chamber pressure,[a] P_0	1.4-4.5 mm Hg	3.6 mm Hg
Droplet diameter, d	50-600μ	300μ
Droplet velocity, v	60-0 ft/s[b]	50 ft/s
Evaporant flow rate	50 lb_m/h	50 lb_m/h
Evaporant temperature[c]	70-75°F	70°F
Surface temperature[d]	35-142°F	65°F
Droplet Reynolds number	4-0[b]	2
Droplet Weber number	2600-0[b]	900

[a] Triple-point pressure of water is 4.58 mm Hg.

[b] Small droplets (less than 100μ) decelerate rapidly due to aerodynamic drag [see Eq. (14)].

[c] Initial water temperature before droplet formation.

[d] Triple-point temperature of water is 32°F.

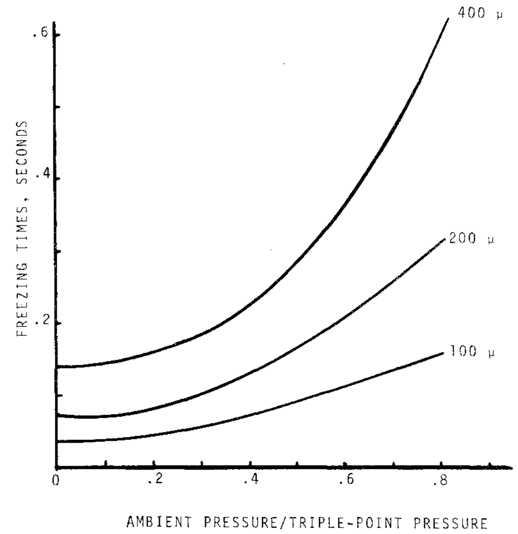

Fig. 1 Water droplet freezing times as a function of the relative pressure for various droplet diameters.

The Weber number, a parameter which determines the impact mechanism for liquid droplets, is the ratio of the incoming droplet kinetic energy to the resisting energy at impact, i.e.,

$$We = \rho d v^2 / g_c \gamma \tag{11}$$

where ρ, d, v, and γ are the density, diameter, velocity, and surface tension of the liquid droplet. At 50 ft/s the Weber number for a 300μ liquid water droplet is about 900. At values of the Weber number above 80, disintegration and splash back of a liquid droplet usually occurs.[6]

Observations of the impacting droplets at chamber pressures close to the triple-point (all liquid droplets) reveal that droplet disintegration and splash back does occur for most of the droplets. If the chamber pressure is too low relative to the triple-point, the droplet evaporates at such an accelerated rate that the droplet surface becomes completely solidified, with the freezing commencing from the outer surface inward. If the solid ice layer is thick enough to withstand the impact forces, a solid droplet rebound occurs; if it is not, then the partially frozen droplet is shattered on impact. An interesting phenomenon which was observed was an above-surface explosion of a large droplet. The specific volume of ice is slightly lower than the specific volume of liquid water, and since the droplet freezes from the outer surface inward, the liquid core is being continually compressed by the newly formed ice. The internal pressure builds up to a level where the yield point of the solid ice is reached, and the droplet explodes.

At moderate chamber pressures relative to the triple-point (i.e., about 3.7 mm Hg), it was observed that nearly all of the incoming droplets impact without disintegration or splash back (i.e., low Weber number impacts). Thus, at these pressures the impacting droplets behave as if their Weber numbers were about an order of magnitude lower than they should be based on the surface tension of liquid water. This important characteristic is essential for efficient operation of the evaporator, since splash back of the droplets degrades the performance of the system.

At moderate chamber pressure the surface of the droplet is not totally liquid (see Fig. 1). When the droplet is formed as it leaves the spray nozzle, evaporative cooling begins at the outer surfce of the droplet, thereby rapidly reducing the outer surface temperature of the droplet. In order to supply the energy needed for evaporation, heat is transferred from the center of the droplet outward. It can be shown that as long as the center core of the droplet is above the triple-point temperature, heat will be transferred to the surface of the droplet, causing it to remain at the triple-point temperature.

The surface temperature will remain at the triple-point temperature for a period of time, since the surface temperature cannot fall below the triple-point temperature until it is completely solidified. A finite quantity of energy (the heat of fusion) must be transferred at the triple-point temperature before the surface can become solidified; thus, the surface remains at the triple-point temperature for a short period of time during the transfer of this finite quantity of heat. In addition, the evaporation rate is much higher than the sublimation rate, and higher temperature gradients (higher core temperatures) are required to evaporate than to sublimate. As the droplet surface becomes more solidified, sublimation becomes the dominant mode of vaporization, thereby reducing the temperature gradients within the droplet. This raises the surface temperature and melts the ice which is formed. As long as the core of the droplet remains above the triple-point temperature, the droplet is self-regulating and the surface will not become completely solidified. The surface temperature will stay at the triple-point during the self-regulation period.[7]

The liquid-solid surface which exists during this time period has an effective surface tension action well above the actual surface tension of liquid water. This increase in effective surface tension lowers the Weber number into the range where droplet disintegration does not occur. Based on observations, there is a broad range of droplet sizes which are in the liquid-solid surface state at a given chamber pressure. This indicates that the time period for this liquid-solid surface state is relatively long.

The existence of a liquid-solid surface is dependent on the surface temperature reaching the triple-point temperature. This is dependent both on the chamber pressure and the exposure time of the droplet. Thus, this necessary state is system dependent and not absolutely related to the chamber pressure. Therefore, different evaporators will work most effectively at different chamber pressures.

The transport fluid temperature varied between a maximum of 185°F to a minimum of 60°F, with 95°F being the usual test value. The surface temperature during evaporation averaged 142°F for the 185°F transport fluid and oscillated within a ±13°F temperature band. The surface temperature for the 60°F transport fluid was 35°F and varied within a very narrow temperature band with some icing occurring on the surface. For the test value of 95°F, the surface temperature held steady at 65°F. There was no observed change in the impact mechanism for a change in surface temperature over the range of surface temperatures considered in the test. The excess temperature (surface and saturation temperature difference) is well below the range at which a vapor layer would form under the droplet at impact. This phenomenon will begin to occur at excess temperatures in the range of 200°F to 250°F and is also dependent on surface roughness.

The velocity of the incoming droplets affects the impact mechanism in that the Weber number is dependent on the velocity. Also, the droplet deceleration is strongly dependent on droplet size. It is shown below that a fractional change in droplet velocity is inversely related to the droplet diameter squared (due to aerodynamic drag), and since the droplet diameter is directly related to the Weber number, the combined effect of the smaller droplet size and the reduced velocity results in a greatly reduced Weber number, i.e., the Weber number at impact is a very strong function of the diameter.

Due to the relatively small droplet diameters, the Reynolds number of the droplets in flight are about unity; thus, Stoke's equation for the drag on a sphere may be used[8]:

$$\text{Drag} = 3\pi\mu v d \tag{12}$$

where μ is the viscosity of the vapor atmosphere, v is the droplet velocity, and d the droplet diameter. Equating the drag force to the inertia force gives

$$\mathrm{d}v/\mathrm{d}t = -18\mu v/\rho d^2 \tag{13}$$

where ρ is the density of the liquid droplet and t denotes time. Integrating gives the following:

$$v(t) = v(0)\ \exp(-18\mu t/\rho d^2) \tag{14}$$

Equation (14) indicates that the velocity of the droplet varies exponentially as an inverse function of the droplet diameter squared, so that there will be significant changes in velocity for small differences in droplet diameters. Water droplets less than 100μ in diameter will decelerate rapidly, while droplets greater than 300μ will hardly be decelerated at all. This phenomenon was observed during the tests, and in some cases small droplets failed to impact the surface altogether and were carried upward away from the surface by the vapor flow.

Evaporation Mechanism

A droplet which impacts and wets the surface of the evaporator will begin to evaporate at impact. Heat is transferred to the droplet from the surface directly below the impacted droplet. This tends to depress the surface temperature initially. At transport fluid temperature of 185°F surface temperatures were depressed as much as 56°F and oscillated between 155°F and 129°F. The resistance to heat flow occurs at the solid-liquid interface, as well as through the liquid droplet itself. It requires about 25°F of excess temperature to generate a vapor bubble at the liquid-solid interface. Once the bubble begins to form it is self-generating, since the vapor layer increases the thermal resistance. The surface temperature below the droplet and the internal pressure of the bubble increase, thereby promoting bubble growth and a further increase in the thermal resistance.

It was observed that during the formation of the vapor bubble, the droplet diameter increased suddenly, the bubble filled the entire droplet, and the droplet diameter increased by a factor of 2 or 3. The droplet assumed the spherical shape of a large vapor bubble, which continued to grow until it finally burst. A model can be developed to predict this droplet blowoff phenomenon by equating the driving force to the resisting force. The internal pressure of the bubble (saturation pressure) times the crossectional area of the bubble accounts for the driving force which causes the bubble to form and grow,

$$\text{Force} = (\pi d^2/4)\Delta P \tag{15}$$

where ΔP is the difference between the bubble internal pressure and the chamber pressure. The resisting force is the surface tension of the liquid times the bubble perimeter,

$$\text{Force} = \pi d\gamma \tag{16}$$

where γ is the surface tension. Combining Eqs. (15) and (16) gives

$$d \geq 4\gamma/\Delta P \tag{17}$$

The equality sign applies before blowoff occurs while the inequality sign applies just at blowoff. Also, it is noted that

$$\text{surface temperature} > \text{saturation temperature} + 25°\text{F} \tag{18}$$

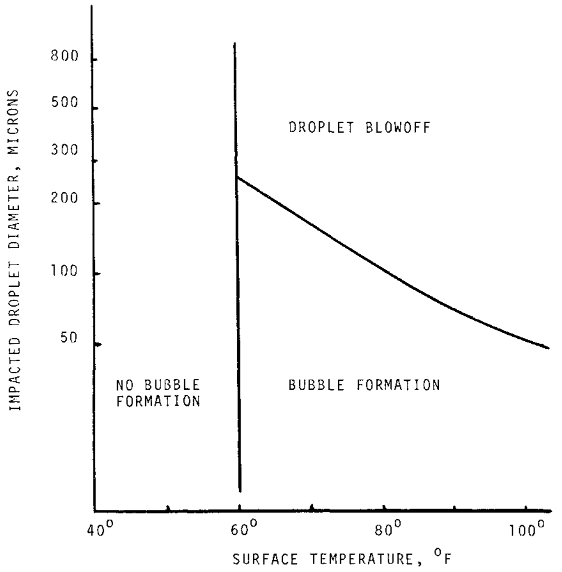

Fig. 2 Evaporating water droplet stability map for various droplet diameters and surface temperatures.

A stability map for water droplet blowoff is plotted in Fig. 2 by combining Eqs. (16) and (17). Referring to Fig. 2, it is seen that if the surface temperature is below 60°F no bubble will form under the droplet and the blowoff will not occur. For temperatures above 60°F the droplet will blow off if the droplet diameter is above the line and will remain on the surface if the diameter is below the line for a given surface temperature. In general, Fig. 2 predicts the types of droplet behavior observed in the photographic study for the range of surface temperature considered during the testing. At the low chamber pressures relative to the triple-point temperature, an ice cap was observed to form on the outer surface of the droplet. This produced in some cases a dramatic blowoff of an ice cap. At the beginning of the bubble formation the droplet was observed to vibrate. The vibration of the droplet decreases the thermal resistance in the vapor layer. The blowoff of the droplet is delayed and in some cases delayed completely. For a low surface temperature and for a small droplet there is very little chance that the bubble diameter would be greater than $4\gamma/\Delta P$, thus the droplet will not blow off the surface. It was observed that blowoff was surface-temperature and droplet-size dependent. The lower the surface temperature and the smaller the droplet, the less likely that blowoff would occur.

The above type of droplet blowoff identifies the surface forces which hold the droplet to the surface. It is therefore possible to estimate the gravitational effects on the droplet at the surface by equating the weight of the droplet to the restraining force, i.e., the surface tension times the droplet perimeter or

$$6\alpha\gamma g_c/d^2\rho g>1 \tag{19}$$

where α is the droplet spreading coefficient, d is the droplet diameter before impact, and ρ is the density. Consider the case where the droplet weight is only 1% of the restraining force; then at 1g the droplet diameter must be less than 980μ to stay on the surface, and in a 2g field it must be less than 695μ. It can therefore be concluded that for water, the droplet restraining forces at the surface are sufficiently high such that in moderate g fields the droplets will not be affected by their own weight.

The evaporation and wetting mechanism were observed to be surface-temperature dependent. At low surface temperatures relative to the saturation pressure, the droplet wets the surface in a favorable manner. The spreading coefficients are large and are predictable from theory. Thus, the ratio of wetted to unwetted surface is relatively high. The evaporation rates are high even though the excess temperatures are low. At moderate surface temperatures a vapor layer forms under the droplet as discussed above. This increases the thickness and decreases the diameter of the droplet. The combined effect of this vapor layer and the lower ratio of wetted to unwetted surface causes the evaporation rates to be low. At high surface temperatures the droplet broke up into a number of smaller droplets, wetting the surface in a more favorable manner and increasing the evaporating rate. This is due in part to the high evaporation rate during the initial spreading of the droplet, as well as the nonuniformity of heat transfer and impacted droplet thickness.

Conclusion

The Weber number, the usual parameter for determining the impact mechanism for a liquid droplet, is not the only parameter to be considered when the ambient pressure is below the triple-point pressure of the liquid. The degree of droplet solidification before impact determines to a large extent the type of impact mechanism that will occur. A liquid-solid droplet surface is an essential requirement for a low-Weber-number type impact, since the surface tension of the liquid water is too low to obtain a low-Weber-number impact at normal spray rates.

A necessary requirement for the existence of a liquid-solid droplet surface is that the droplet surface be at the triple-point temperature. This requirement is determined by several factors, including the chamber pressure, droplet exposure time, droplet size, and to a lesser degree, the droplet initial temperature. Due to the transient nature of the heat transfer, the droplet will stay in this state for a period of time. Thus, it is possible under the proper conditions to have nearly all the droplets of the spray in this state even though the droplet sizes may vary within the spray. Since this necessary state is system dependent and not absolutely related to the chamber pressure, different evaporators will work most effectively at different chamber pressures.

Droplet blowoff is dependent on droplet size and evaporator surface temperature. Gravity does not affect the droplet blowoff phenomenon, since the forces which hold the droplet to the surface are more than an order of magnitude higher than the droplet weight itself.

Acknowledgment

This paper presents the results of research performed while on a NASA-ASEE Summer Faculty Fellowship at the Johnson Spacecraft Center in Houston, Texas.

References

[1] Bell, K.J., "The Leidenfrost Phenomenon: A Survey," *Chemical Engineering Progress Symposium Series,* Vol. 63, No. 79, 1967, pp. 73-82.

[2] Baumeister, K.J. and Simon, F.F., "Leidenfrost Temperature – Its Correlations for Liquid Metals, Cryogens, Hydrocarbons and Water," *Journal of Heat Transfer, Transactions of the ASME,* Vol. 95, May 1973, pp. 166-172.

[3] Toda, S., "A Study of Mist Cooling (Part 4)," *5th Japan Heat Transfer Symposium,* 1968, pp. 265-268.

[4] Toda, S. and Uchida, H., "A Study of Mist Drops on a Heated Surface at High Temperatures and High Heat Fluxes," *Fourth International Heat Transfer Conference,* Paris – Versailles, 1970.

[5] Gayle, J.B., Egger, C.T., and Branstord, J.W., "Freezing of Liquids on Sudden Exposure to Vacuum," *Journal of Spacecraft and Rockets,* Vol. 1, May-June 1964, pp. 323-326.

[6] Wachters, L. and Westerling, N., "The Heat Transfer from a Hot Wall to Impinging Water Drops in the Spheroidal State," *Chemical Engineering Science,* Vol. 21, Dec. 1966, p. 1231-1238.

[7] Cho, S.H. and Sunderland, J.E., "Phase Change of Spherical Bodies," *International Journal of Heat and Mass Transfer,* Vol. 13, 1970, pp. 1231-1233.

[8] Schlichting, H., *Boundary-Layer Theory,"* McGraw Hill, New York, 1968, p. 106.